Electronic Supplementary Material (ESI) for Soft Matter

A simple approach to characterising block copolymer assemblies: graphene oxide supports for high contrast multi-technique imaging

Joseph P. Patterson, Ana M. Sanchez, Nikos Petzetakis, Thomas P. Smart, Thomas H. Epps III, Ian Portman, Neil R. Wilson, Rachel K. O'Reilly**

The supporting information provides additional information on the synthesis and self assembly of the polymers and includes images to back up and further develop the work discussed in the main article.

Materials

All chemicals were used as received from Aldrich, Fluka, or Acros unless otherwise stated. *Tert*-butyl acrylate and styrene monomers were distilled over CaH_2 prior to use and stored at 5°C. AIBN [azobisisobutyronitrile] was recrystallized twice from methanol and stored in the dark at 5 °C. DDMAT [S-dodecyl-S'-(α',α'-dimethyl-α''-acetic acid)],[1] polylactide$_{40}$-*b*-polyacrylic acid$_{286}$ cylindrical micelles (**5**)[2] and solutions of graphene oxide[3] were synthesized as previously reported. Copper TEM grids were purchased from Agar, stained images were obtained on 300 mesh formvar/carbon grids, GO imaging was performed on 400 mesh lacy carbon films with deposited GO films and cryo-TEM images were on Quantifoil holey carbon grids with 200 mesh.

Instrumentation

^{1}H NMR spectra were recorded on a Bruker DPX-400 spectrometer in $CDCl_3$. Chemical shifts are given in ppm downfield from TMS. Size exclusion chromatography (SEC) measurements were conducted on a system comprised of a Varian 390-LC-Multi detector suite fitted with differential refractive index (DRI), light scattering (LS), and ultra-violet (UV) detectors equipped with a guard column

(Varian Polymer Laboratories PLGel 5 µM, 50 × 7.5 mm) and two mixed D columns (Varian Polymer Laboratories PLGel 5 µM, 300 × 7.5 mm). The mobile phase was tetrahydrofuran with 5% triethylamine eluent at a flow rate of 1.0 mL min^{-1}, and samples were calibrated against Varian Polymer laboratories Easi-Vials linear poly(styrene) standards (162 - 2.4 × 10^5 $g.mol^{-1}$) using Cirrus v3.3 software. Infrared spectroscopy was recorded on a Perkin-Elme, Spectrum 100 FT-IR spectrometer.

Cryogenic transmission electron microscopy (cryo-TEM) samples were prepared at 25 °C using a FEI 110 Vitrobot to maintain a constant humidity environment. A droplet of 2-10 µL of sample solution was added to a holey carbon-coated copper grid, and the grid was blotted to remove excess solution. The grid was subsequently plunged into liquid ethane to vitrify the sample. Grids were transferred to a Gatan cryo stage and imaged at 120 keV using a Tecnai G2 12 Twin TEM equipped with a Gatan CCD camera. The temperature of the cryo stage was maintained below -170 °C during imaging. GO and stained TEM images were recorded on either a JEOL 2000FX TEM or a JEOL 2100 equipped with Gatan Orius digital camera, both were operated at 200kV. Unless otherwise stated, images were acquired under conventional bright-field conditions. Tomography was carried out on a JEOL 2010F with a Gatan Ultrascan 4000 camera at 200 kV tilting from -42° to +42° in 2° increments. Images were acquired using Mr.T[4] software and reconstructed with SIRT (Simultaneous Iterative Reconstructive Technique) algorithm, 30 iterations with a relaxation coefficient of 1. ImageJ[5] and TomoJ[6] were used for processing, and the surface rendering after a manual segmentation process was undertaken using Amira software.

AFM images were taken in tapping mode on a Multimode AFM with Nanoscope IIIA controller with Quadrex, or an Asylum Research MFP3D-SA. Silicon AFM tips were used with nominal spring constant and resonance frequency of 3.5 Nm^{-1} and 75 kHz (MikroMasch NSC18).

A Zeiss Supra55VP was used to acquire the SEM images, operated at an accelerating voltage of 20 kV.

Methods

Synthesis of P^tBuA_{11} (1)

DDMAT (0.14 g, 3.9 mmol), P^tBuA (1.0 g, 7.8 mmol), azobisisobutyronitrile (AIBN) (6.4 mg, 0.39 mmol) and dioxane (1.14 mL) were added to a clean dry ampoule under N_2 and stirred until homogeneous. The solution was degassed *via* 3 freeze-pump-thaw cycles and placed under N_2. The

solution was heated to 65 °C for 45 min and then quenched in liquid N_2. The viscous solution was dissolved in the minimum amount of THF, and the polymer was precipitated into a mixture (by volume) of 7:1 cold MeOH:H_2O. The MeOH:H_2O solution was decanted, and the polymer was dissolved in THF and then dried over $MgSO_4$. Then, the polymer was filtered and the solvent removed *in vacuo* affording polymer **1**. M_n (^{1}H NMR) = 1.8 kDa, M_n (SEC) = 1.7 kDa, M_w/M_n (SEC) = 1.09.

Chain extension of (1) with styrene to give P*t*BuA$_{11}$-*b*-PS$_{190}$ (2)

1 (0.027 g, 15 µmol) and styrene (0.70 ml, 6.1 mmol) were added to a clean dry ampoule under N_2 and stirred until homogeneous. The yellow solution was degassed *via* 4 freeze-pump-thaw-cycles and placed under N_2. Then, the solution was then heated to 110 °C for 22 h and quenched with rapid cooling into liquid N_2. The viscous solution was dissolved in the minimum amount of THF, and the polymer was precipitated three times into cold MeOH. The polymer was filtered and dried *in vacuo*. M_n (^{1}H NMR) = 21.5 kDa, M_n (SEC) = 25.9 kDa, M_w/M_n (SEC) = 1.08.

Conversion of P*t*BuA$_{11}$-*b*-PS$_{190}$ (2) to PAA$_{11}$-*b*-PS$_{190}$ (3)

2 (58.4 mg) was added to a small vial and dissolved in dichloromethane (3 mL). The solution was stirred at 0 °C for *ca.* 30 min and trifluoroacetic acid (1.0 mL) was added dropwise over *ca.* 10 min. The solution was stirred and allowed to warm to room temperature overnight. All volatiles were blown off with N_2. The remaining solid was dissolved in the minimum amount of THF, and the polymer was precipitated twice into cold MeOH. The polymer was filtered and dried *in vacuo*. ^{1}H NMR, 400 MHz ($CDCl_3$): δ (ppm) 7.25-6.25 (m br, 5H Ar polymer), 2.36-0.89 (br, CH and CH_2 polymer backbone). IR (ν_{max}/cm^{-1}): 1943, 1872, 1803, 1713, 1601, 1584, 1493, 1451, 1370, 1181, 1154 (weak), 1069, 1028, 964, 906.

Self-Assembly of (3)

3 (8.0 mg) was added to a vial and dissolved in DMF (4.0 mL). The solution was stirred for *ca.* 30 min before the dropwise addition of nanopure water (4.0 mL) over *ca.* 60 min using a peristaltic pump. Then, the solution was dialyzed (using 3.5 kDa MWCO tubing) against 2 L of nanopure water with 3 water changes. The final polymer concentration in solution was 0.65 mg mL^{-1}

Synthesis and Self-Assembly of PAA_{100}-b-PS_{46} (4)

4 was synthesized by an analogous method to **3** by varying the equivalents of *t*BuA and styrene. For self-assembly, **4** (4.0 mg) was added to a vial and dissolved in DMF (4.0 mL). The solution was stirred for ca. 2 h before the dropwise addition of nanopure water (4.0 mL) over *ca.* 60 min using a peristaltic pump. Then, the solution was dialyzed (using 3.5 kDa MWCO tubing) against 2 L of nanopure water with 3 water changes. The final polymer concentration in solution was calculated to be 0.3 mg mL^{-1}.

Artifacts observed during analysis of the samples in the article using staining TEM techniques

One of the key aspects in the paper is the difficulty which can occur when analyzing TEM images of block copolymer assemblies using high electron absorbing stains. Fig. S1 shows a representative TEM image of PAA_{11}-*b*-PS_{250} polymersomes stained with PTA and it is clear that no real membrane structure can be distinguished which is the main indicator for polymersome formation. Another artifact is highlighted by the red circle, which shows a large number of small spherical structures, which were not seen in either the GO or cryo TEM images. As well as hiding structures on the grid stains can also introduce structure which is not actually present in the sample. For example, Fig. S2 shows a TEM image of PAA_{100}-*b*-PS_{40} spherical micelles with PTA stain where the stain had created a ring like structure in the particles similar to that observed for the membrane layer in polymersomes.

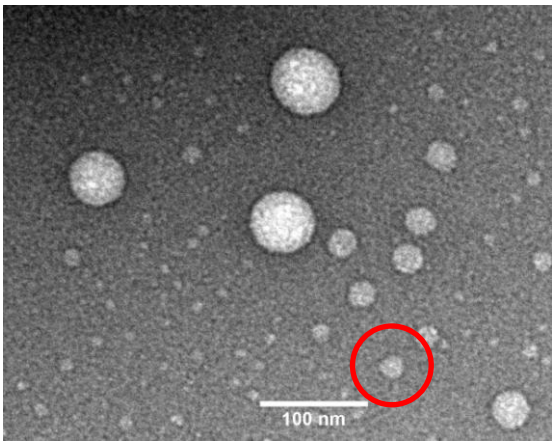

Fig. S1. Representative TEM image of PAA_{11}-*b*-PS_{250} polymersomes stained with PTA.

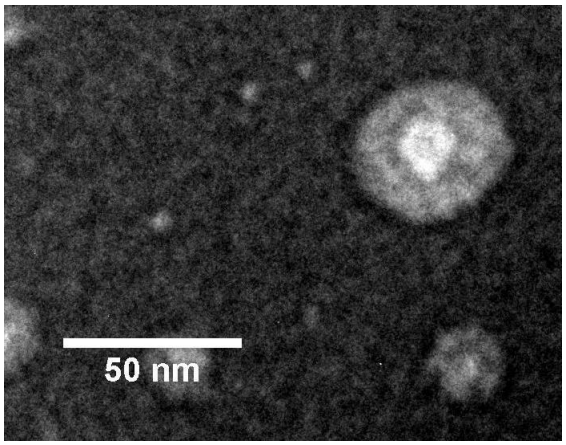

Fig. S2. Representative TEM image of PAA_{100}-*b*-PS_{40} polymersomes stained with PTA.

PAA_{100}-b-PS_{46} spherical micelles

Table S1 highlights that the average diameters measured by TEM for a range of different staining techniques and unstained GO samples are consistent. Whilst, Fig S3 shows a representative AFM image for the PAA_{100}-*b*-PS_{46} spherical micelles imaged directly on the GO TEM grid. We propose that using GO as a substrate for TEM also allows for the simple and quick characterization of the 3D nature of the particles using AFM analysis. This is not possible on stained TEM samples or cryo-TEM samples. Comparing this height information to the average diameter information obtained by TEM indicates as expected there is significant distortion of the particles when dried to a surface. However, an advantage of this approach is that particles can be imaged both in 2D and 3D on the same substrate to allow for the elimination of different drying effects which are often reported for particles imaged using TEM and AFM characterization.

Table S1. Summary of the measurements made for the same PAA_{100}-*b*-PS_{46} spherical micelle solution using a range of imaging techniques.

Technique	Average Diameter[a] (TEM) / nm	Average Height[b] (AFM) / nm
UA Staining	24 (±5)	n/a
AM Staining	20 (±4)	n/a
PTA staining	22 (±4)	n/a
GO	23 (±4)	10 (±3)

[a]100 particles counted, [b]16 particles counted.

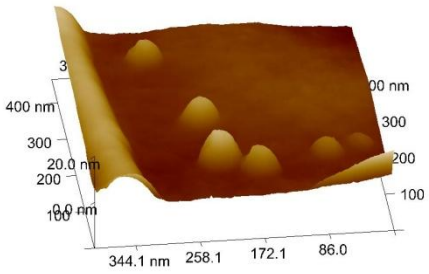

Fig. S3 Representative AFM image of the PAA_{100}-*b*-PS_{46} spherical micelles imaged directly on the GO TEM grid.

Multilamella structures present in sample PAA_{11}-b-PS_{190} (4)

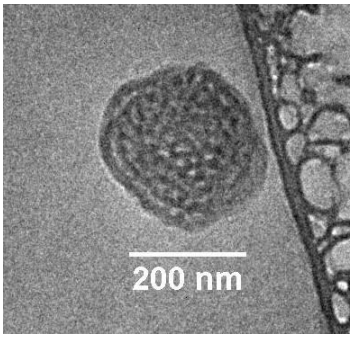

Fig. S4 Representative cryo-TEM image of multilamellar structures present in the PAA_{11}-*b*-PS_{190} sample (**4**).

Fig. S4 shows a cryo-TEM image of one of the multilamellar structures present in sample (**4**), such structures have been previously reported in related systems by Eisenberg. This data highlights that these structures are present in solution and not an aggregation of multiple polymersomes which could occur when drying the sample to a surface. This is especially important to consider when analyzing our samples in the dried state on GO compared to cryo-TEM analysis in the native state.

Tuning the hydrophobicity of GO for organic assemblies

The block copolymer assemblies studied in the article were all aqueous based samples. The hydrophilic nature of GO is ideal for readily absorbing these samples however, there is also interest in the preparation and characterization of block copolymers in organic solutions. However, the analysis of assemblies from organic solvent by cryo-TEM is very challenging. TEM analysis of an organic based polymeric assembly has already been reported by our group[7] showing GO TEM grids can also be used for these samples deposited from chloroform. In Fig. S5 we highlight that should it be required hydrophobicity can be dialled into the GO substrate once it has been deposited on a surface by simply heating the TEM grids for 1 hour at various temperatures. In Fig. S5 the increase in water contact angle of a GO thin film with respect to heating temperature are reported. These measurements were carried out by spin casting GO (*ca*. 1.5 mg mL^{-1}) onto SiO_2 chips (initial contact angle ca. 65°) which were placed on a hot plate for 1 hour at the corresponding temperature. Following this 10 mL of water was pipetted onto the surface for contact angle measurements.

GO 50°C 1hr 75°C 1hr 100°C 1hr 200°C 1hr

ca. 12° *ca.* 90°

Fig. S5 Pictures shows the increasing contact angles of a GO thin film with respect to increasing heating temperature.

Polylactide-b-poly acrylic acid ($PLLA_{40}$-b-PAA_{286}) (5) cylinders

Fig. S6 left panel, shows a representative AFM image of the cylinders recorded directly on the GO TEM grid. As discussed in the article the cylinder cores appear to hold their shape when dried to the GO surface indicating that they are indeed solid in nature. Fig. S6 right panel, shows a representative SEM image of the cylinder on the GO TEM grid which was recorded after deposition of a thin layer of Au onto the surface of the grid, following both TEM and AFM analysis. This deposition was performed in order to protect the sample from contamination or damage by the electron beam, however when analyzing the PAA_{11}-*b*-PS_{190} polymersomes (**4**) on the finder grid withouth any coating (Fig.7, main article) little contamination or damage occurred to the sample, suggesting this coating may not be necessary.

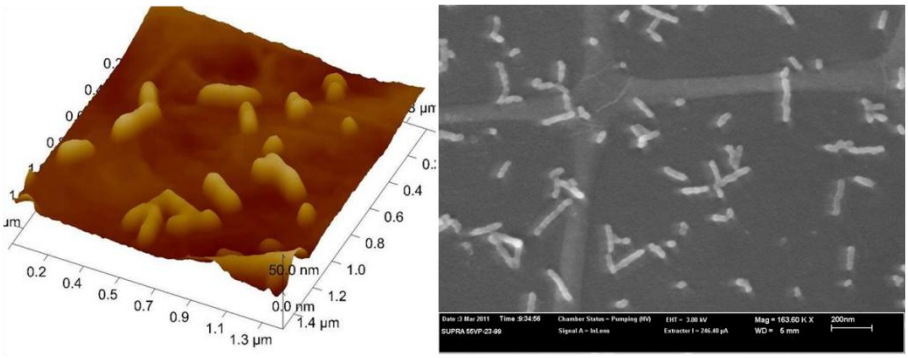

Fig. S6 Representative AFM (left) and SEM (right) of ($PLLA_{40}$-*b*-PAA_{286}) (**5**) cylinders.

Finder grid images for the PAA_{11}-b-PS_{190} polymersomes (4)

Fig. S7 (top row) shows lower magnification images of the area where the TEM, AFM and SEM images of the same particles were recorded (Fig. S7 bottom and Fig. 7, main article). One interesting feature of the AFM image (centre, bottom) is that the GO appears to be distorted around the area containing the three particles touching each other (just below and to the left of the center image). These distortions cannot be seen in either the TEM of SEM images (Figs. S7 or S8). The AFM image recorded from the same area of the grid but on the reverse side (Fig. S8 left), shows that even the smaller particles in the image have created distortions on the GO as small bumps can be seen where the particles are attached to the opposite side of the GO sheet. This indicates a strong affinity of the particles for the GO and is probably due to H-bonding interactions between the acrylic acid corona of the polymersomes and the oxygenated surface of the GO.

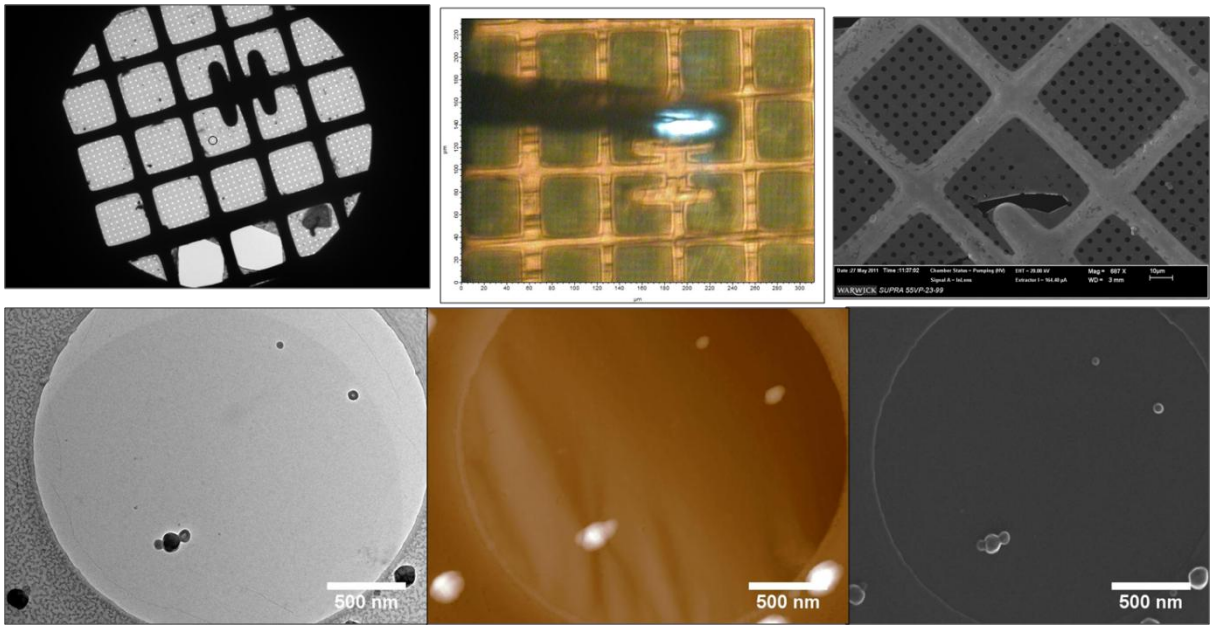

Fig. S7 Finder grid images from TEM (left), the optical microscope on the AFM (centre, top) and the SEM (right) showing the same area from which the data using all 3 techniques was collected.

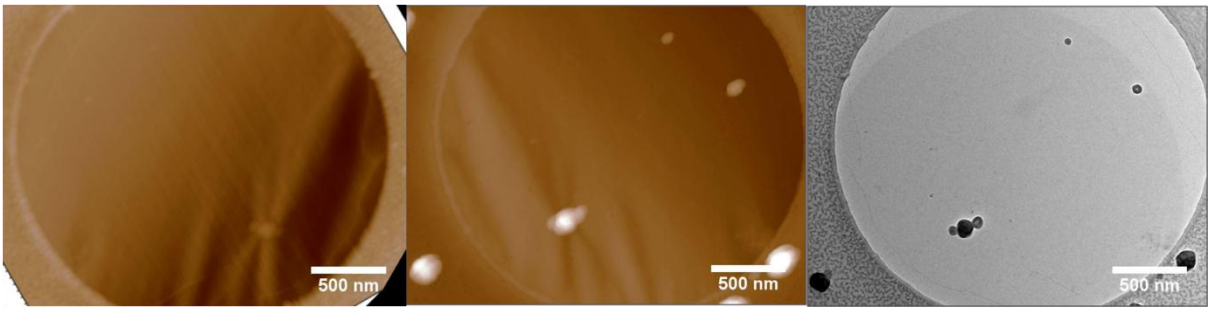

Fig. S8 AFM images of the GO TEM grid on the reverse side to where the particles were deposited (left) and the corresponding AFM images on the side where the particles were deposited (centre) and TEM image (right) of the same area.

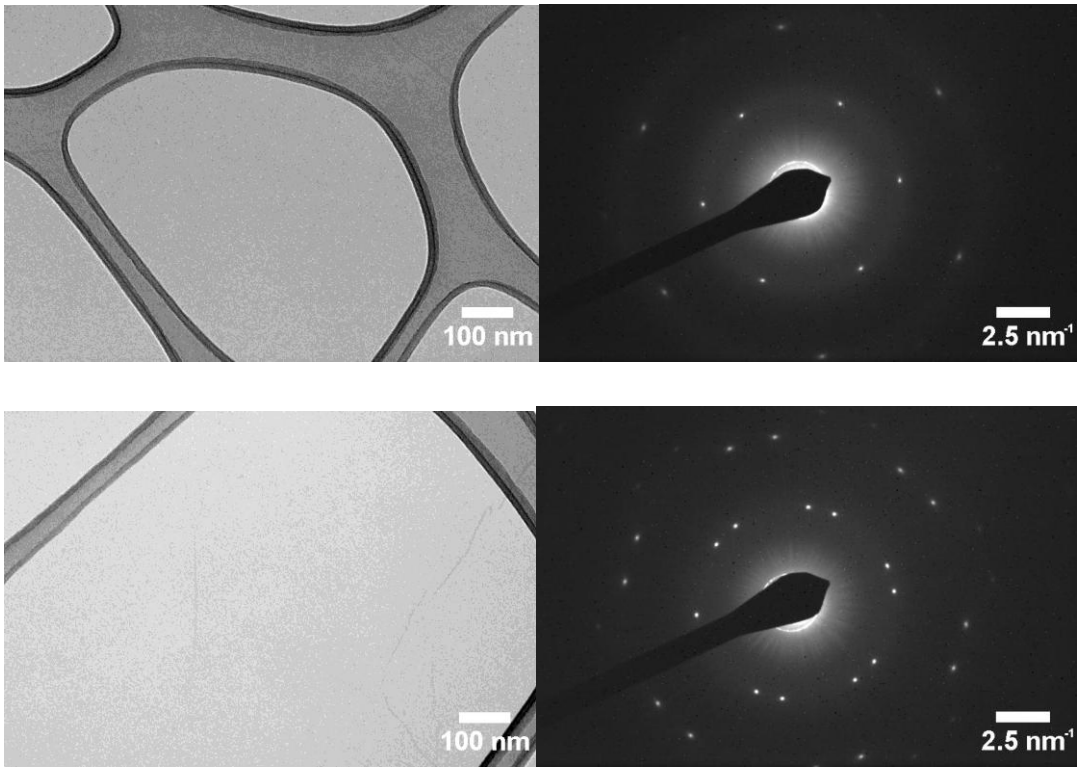

Fig. S9 Bright field images (left) and corresponding diffraction patterns (right) for and area of single (top) and double (bottom) sheet GO.

References

1. Skey, J.; O'Reilly, R. K. *Chem. Commun.* **2008**, (35), 4183-4185.

2. Petzetakis, N.; Dove, A. P.; O'Reilly, R. K. *Chem. Sci.* **2011,** 2, (5), 955-960.

3. Wilson, N. R.; Pandey, P. A.; Beanland, R.; Young, R. J.; Kinloch, I. A.; Gong, L.; Liu, Z.; Suenaga, K.; Rourke, J. P.; York, S. J.; Sloan, J. *ACS Nano* **2009,** 3, (9), 2547-2556.

4. Chang, J. T.; Marsh, M.; Rixon, F.; Chiu, W. *Microscopy and Microanalysis* **2005,** 11, , 308-309.

5. Abramoff, M. D., Magelhaes, P.J., Ram, S.J. *Biophotonics Inter.* **1997-2011,** 11, (7), 36-42.

6. Messaoudil, C.; Boudier, T.; Sorzano, C. O. S.; Marco, S. *BMC Bioinformatics* **2007,** 8.

7. Williams, P. E.; Moughton, A. O.; Patterson, J. P.; Khodabakhsh, S.; O'Reilly, R. K. *Polym. Chem.* **2011,** 2, (3), 720-729.